# Single molecules in soft matter : a study of biomolecular conformation, heterogeneity and plasmon enhanced fluorescence

Yuan, H.

# 5 Individual gold nanorods report on dynamical heterogeneity in supercooled glycerol

**Abstract** –Building upon previous reports of dynamical heterogeneity in supercooled glycerol probed with single dye molecules, we have investigated the rotational diffusion in glycerol of much larger objects, single gold nanorods. Because of their size and much larger hydrodynamic volume, nanorods probe very different length and time scales than dyes. They are best suited for studies around the critical temperature of glycerol. Our results show that heterogeneity appears at temperatures lower than 225 K, even on the length scale of 30 nm, the averaged size of the nanorods. Moreover, the persistence of heterogeneity on the measurement time scale proves that the exchange times are much longer than the rotation time of the rods.

The contents of this chapter have been accepted for publication:
H. Yuan, S. Khatua, P. Zijlstra, and M. Orrit.
*Faraday Discuss.* (DOI): 10.1039/C3FD00091E.

## 5.1 Introduction

Supercooled liquids have drawn much attention because of the fundamental importance of the glass transition, and because of the ubiquitous technological applications of glasses and amorphous materials. It is now widely accepted that, at temperatures close to their glass transition, supercooled liquids, while remaining amorphous, become heterogeneous [53–55, 165]. Heterogeneity is believed to be a key element for a deeper mechanistic understanding of the glass transition of supercooled liquids. Although first observed in various bulk experiments [63–65, 93, 144, 145, 166, 167], heterogeneity in supercooled liquids remains difficult to observe and characterize at the ensemble level. In particular, the spatial and temporal scales associated to heterogeneity in supercooled liquids are still in debate. In simple glass-forming molecular liquids such as glycerol and *o*-terphenyl, different spatial and temporal scales have been reported in different bulk experiments. Nuclear magnetic resonance (NMR) and dielectric relaxation experiments indicate heterogeneity on a length scale of several nanometers and a time scale comparable to the alpha-relaxation time [164, 166–170]. On the contrary, light scattering and fluorescence microscopy experiments indicate heterogeneity on length scales up to several hundred nanometers and orders of magnitude slower relaxation [148, 171–173]. Without a clear agreement on the spatial and temporal scale(s) of heterogeneity, deeper mechanistic questions will remain open. Therefore, we have undertaken this study of rotational diffusion of nanoparticles to explore larger length and time scales in the hope of directly accessing the local properties of glass-forming liquids at molecular and nanometer scales.

Suppressing ensemble averaging, single-molecule studies on fluorophores doped in supercooled liquids started to provide detailed information at a molecular level [32, 33, 56]. Tracking rotational motions of individual molecules embedded in supercooled *o*-terphenyl, Deschenes and Vanden Bout found a broad distribution of molecular tumbling rates and revealed the heterogeneity experienced by single molecules [57]. In experiments on glycerol, Zondervan *et al.* found that the memory time of heterogeneity could exceed by many orders of magnitude the relaxation time of individual glycerol molecules [58]. These surprisingly long times may have been a consequence of the thermal history of that particular experiment, but in a more recent work, Mackowiak *et al.* have confirmed the presence of temporal heterogeneity with a memory time two orders of magnitude longer than the tumbling time of glycerol molecules [59]. These observations suggest the existence of slowly relaxing regions, or even of solid-like networks within supercooled liquids close to the glass transition. Moreover, these studies reveal that these structures persist well above

the structural glass transition temperature of glycerol (190 K). A study of the tumbling rates of the molecules suggests the disparition of heterogeneity at a temperature of about 230 K for glycerol [58], tentatively close to the cross-over temperature ($T_c$) predicted theoretically by mode-coupling theory [53, 67, 68]. A direct experimental demonstration of the merging of heterogeneous environments into a single liquid at $T_c$, however, could not be achieved in these first experiments because of the very fast rotational diffusion of the probe dye molecules at that high temperature, compounded by the inherent blinking and bleaching of single molecules. Hence, gold nanorods, which offer much larger volume and perfect photo-stability, are attractive probes of heterogeneities at higher temperatures.

The original properties of gold nanorods make them very attractive probes of heterogeneity on large length and time scales. First of all, they are easy to detect one by one thanks to the strong interaction of their longitudinal plasmon resonance with light. They have a much larger volume than single molecules and this volume can be easily tuned by chemical synthesis [69, 174]. They do not blink nor bleach and thus can be detected continuously for practically unlimited times. They are easily detected optically, either by scattering [175, 176], by absorption [177], or by luminescence (one-photon- and two-photon-excited) [178, 179]. Although its quantum yield is very low [70], one-photon-excited luminescence of single gold nanorods is easily detected because of their large absorption cross-section. Moreover, the anisotropic shape of gold nanorods makes their optical response sensitive to orientation and is thus a direct probe of their rotational diffusion.

In the present work, we propose the use of individual gold nanorods as local viscosity reporters for studying the dynamics of glass-forming liquids. This demonstration experiment allows us to follow the rotational diffusion times of individual gold nanorods from 238 K to 222.5 K. The rotational diffusion time of a nanorod is deduced from autocorrelation functions of the linear dichroism provided by one-photon luminescence time-traces. We first measure the gold nanorods' rotational times at high temperature, where glycerol still appears homogeneous. While cooling, we follow the rotational times of the same gold nanorods at different temperatures and compare their rotational times with calculations based on the bulk viscosity of glycerol.

Glycerol of spectrophotometric grade was purchased from Sigma-Aldrich and used without further purification. Gold nanorods were prepared with the seed-mediated growth method as described in the literature [180]. The gold nanorods used in this study had averaged dimensions of 14 nm × 35 nm, and are depicted in the SEM micrograph of figure 5.1 (a). Their longitudinal plasmon

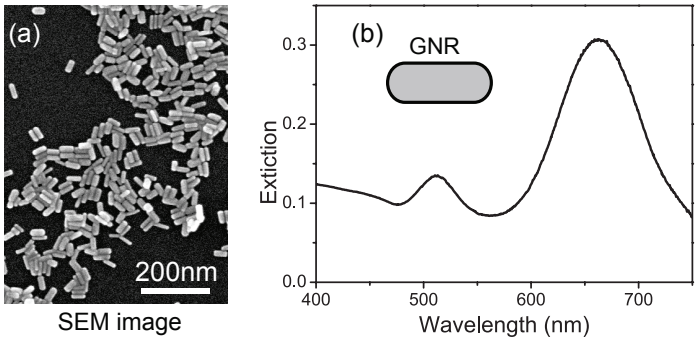


**Figure 5.1:** (a) A SEM image of the gold nanorods (14±3 nm×35±5 nm). (b)The UV-Vis spectrum of gold nanorods in water. It shows two plasmon resonances. The one around 650 nm is the longitudinal surface plasmon resonance. The other one around 520 nm is the transverse surface plasmon resonance.

resonates around 650 nm in water, as shown in 5.1 (b). The gold nanorods were then dispersed into glycerol by first washing them, i.e., by removing the excess amount of cetyl-trimethylammonium bromide (CTAB) through centrifugation and redispersion into MilliQ water, followed by subsequent dilution with glycerol to a volume ratio of 1:400 (water: glycerol). The gold nanorod suspension was then spin-coated onto an ozone-cleaned glass coverslide at 6000 rpm for 60 seconds, yielding a film of 2 - 3 $\mu m$ thickness. We then mounted the sample into the cryostat of our home-built beam-scanning confocal microscope. The position of the sample is controlled by a three-dimensional set of piezo-stages with feedback loop. Before cooling down, the sample was dried in the cryostat by repeatedly pumping and flushing with helium gas. Furthermore, we kept it under a dry and inert helium atmosphere throughout the entire experiment. The sample was directly cooled down to 238 K with a cooling rate of 5 K per hour. We followed the same gold nanorods at 238 K, 235 K, 232 K, 229 K 226 K and 222.5 K. During each measurement, the temperature inside cryostat was regulated within ±0.1 K. Previous experiments [66, 148, 181] have shown that glycerol subject to such a thermal history remains amorphous, with no sign of nano-crystallites.

Single-particle measurements were performed on a home-built confocal laser-scanning microscope with the objective lens inside a flow cryostat. The detailed description of the experimental setup can be found elsewhere. [51,115]

A simplified scheme of the optical setup is shown in figure 5.2. A 633 nm He-Ne laser was used as the excitation source. The circularly polarized excitation beam was focused into the glycerol film through a fused-silica objective with a numerical aperture of 0.82. The photoluminescence signal was collected by the same objective and was separated from the excitation laser using a 633 nm notch filter. For polarization-sensitive measurements, the photoluminescence signal from the individual gold nanorods was split by a polarizing beam-splitter and then detected by two single-photon avalanche photodiodes (APDs) for the two orthogonal polarizations. Photoluminescence spectra were recorded by a liquid-nitrogen-cooled CCD spectrometer (Horiba Scientific).

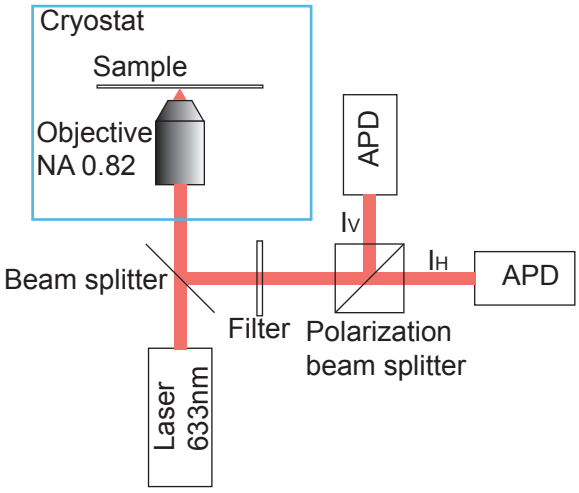


**Figure 5.2:** Simplified scheme of the optical setup. Circularly polarized laser excitation at 633 nm is sent into the cryostat and then focused into the sample film by a fused-silica objective with a NA of 0.82. Photoluminescence from gold nanorods is collected by the same objective. After the 633 nm notch filter, the photo-luminescence is split into two parts according to polarization. Two Perkin-Elmer APDs are employed to measure the intensities in each channel.

## 5.2 Results

Figure 5.3 (a) shows a typical photoluminescence image of individual gold nanorods dispersed in glycerol. To make sure that the bright spots on the image stem from individual gold nanorods, we measured their photoluminescence spectra.

A few typical spectra are shown normalized in figure 5.3 (b). A Lorentzian lineshape with narrow linewidth (34±2 nm) confirms that each spot indeed arises from a single gold nanorod. Although scattering spectra are more commonly used in the literature to identify single nanorods against clusters, we have recently shown that luminescence spectra of gold nanorods closely resemble their scattering spectra and thus can be used as well for identification [70]. All measurements in this work were performed on single gold nanorods which were identified by their photoluminescence spectra. We note that there is a broad distribution of intensities among the bright spots even though they are all single gold nanorods. This intensity distribution results from two factors. (i) The nanorods produced by the chemical synthesis may have different volumes. This is supported by the SEM image of Fig. 1a. (ii) The surface plasmon resonances of the individual nanorods, related to their aspect ratio, are also distributed, leading to a distribution of absorption cross sections at the excitation wavelength. The latter effect is particularly important as the excitation laser wavelength (633 nm) is close to the surface plasmon resonance (SPR) of the bulk nanorod sample.

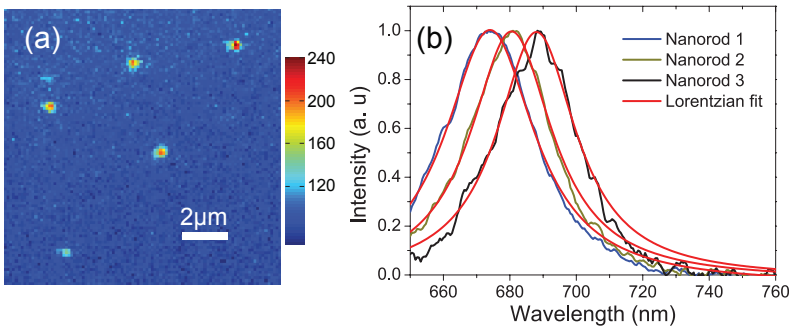


**Figure 5.3:** (a) One-photon-excited luminescence image of individual gold nanorods dispersed in glycerol at 232 K. The excitation wavelength was 633 nm and the power density was 10 kW/cm$^2$. (b) Three examples of photoluminescence spectra of the bright spots in (a). The narrow Lorentzian line-shape of their spectra identifies the emitters as individual gold nanorods.

We note that individual nanorods in figure 5.1 (a) are not stationary. This is quite evident from their photoluminescence time traces measured along two orthogonal polarizations. A typical photoluminescence time trace is shown

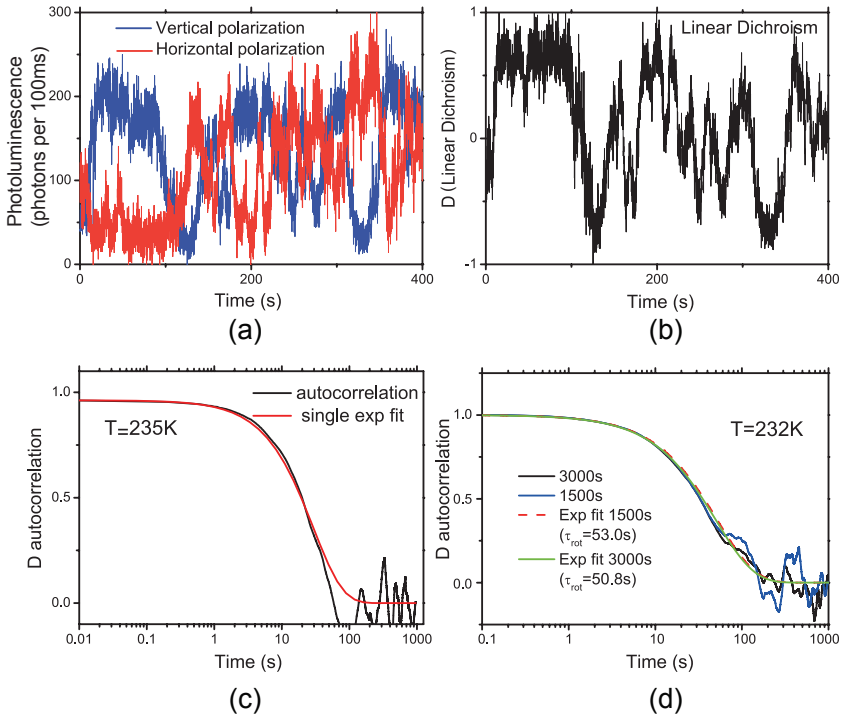


**Figure 5.4:** (a) Typical photo-luminescence intensity time trace of a single gold nanorod rotating in supercooled glycerol. The excitation intensity of circularly polarized 633 nm excitation light was 200 W/cm$^2$. The integration time was 100 ms. Blue and red traces represent the intensities of the two orthogonal polarizations. (b) The linear dichroism trace calculated from (a) according to equation (5.1). (c) Autocorrelation of the linear dichroism trace shown in (b). A single-exponential fit (red) yields a rotational correlation time of 24 s at 235 K. (d) Autocorrelation of linear dichroism traces of different lengths recorded for the same gold nanorod at 232 K. The blue curve is from a 1500 s timetrace yielding a rotational correlation time of 53 s (the red dashed line). The black curve is from a 3000 s timetrace yielding a rotational correlation time of 50.8 s (the green line).

in figure 5.4 (a). The anti-correlated intensity fluctuations along the orthogonal polarizations directions clearly indicate in-plane rotation of individual nanorods. Fluctuation of the total intensity is related to the out-of-plane motion of the nanorods. To quantify the rotational diffusion of the nanorods, we calculate the linear dichroism ($D$) from the photoluminescence time-trace

using the following equation:

$$D = \frac{I_H - I_V}{I_H + I_V}, \tag{5.1}$$

where $I_H$ and $I_V$ are the intensities of horizontal and vertical polarizations, respectively. Figure 5.4 (b) shows the linear dichroism time trace calculated from the polarized photoluminescence time trace shown in figure 5.4 (a). We note that, even though linear dichroism only characterizes the in-plane projection of the long axis of the nanorods, the rotational diffusion times can be deduced from this two-dimensional projection linear dichroism, assuming that the nanorods' diffusion is isotropic [57].

As in single-molecule experiments, we deduce rotational diffusion times of individual nanorods from the autocorrelation of the linear dichroism time-traces [58]:

$$C'_D = \frac{\langle (D(t'+t)+1)(D(t')+1)\rangle}{\langle D(t')+1\rangle^2} - 1 \approx \frac{1}{2}\exp(-\frac{t}{\tau_{rot}}). \tag{5.2}$$

The autocorrelation is then fitted with a single-exponential decay, where $\tau_{rot}$ is the rotational correlation time. Figure 5.4 (c) (black) shows the autocorrelation of the linear dichroism time trace shown in figure 5.4 (b) (note the logarithmic time axis). The single-exponential fit of equation (5.2) yields a rotational diffusion time of 24 seconds at 235 K. It is known that the finite length of linear dichroism time-trace can affect the fitted diffusion time, and in particular that a too short measurement time leads one to incorrectly estimate the diffusion time [59, 182]. Therefore, to check the reliability of our procedure, we compared the recovered rotational diffusion times for two linear dichroism time traces acquired on the same nanorod for different durations. Figure 5.4 (d) shows examples of linear dichroism autocorrelation functions acquired on the same rod for durations of 1500 (blue line) and 3000 (black line) seconds. The fitted rotational diffusion times are 53 seconds (for 1500 seconds, $30\tau_{rot}$) and 50.8 seconds (for 3000 seconds, $60\tau_{rot}$) respectively. From such measurements on several nanorods we estimate that the uncertainty in the recovered rotational diffusion time is at most $\pm 15\%$ provided that the time traces are longer than 30 times $\tau_{rot}$ [59]. All further measurements of linear dichroism traces were done on time traces at least 50 times longer than the measured rotational diffusion time. Such measurements can require hours and were possible only thanks to the exceptional photostability of gold nanorods. Individual nanorods could be followed easily over such long times because translational diffusion through the focal spot was very slow, almost three orders of magnitude slower than rotational diffusion.

The rotational diffusion time of a nanorod can be directly related to the local viscosity it experiences via the Debye-Stokes-Einstein relation:

$$\tau_{rot} = \frac{V_h \eta}{k_B T} \tag{5.3}$$

with $V_h$ the hydrodynamic volume of nanorods, $\eta$ the local viscosity, $k_B$ Boltzmann's constant and $T$ the temperature. Hydrodynamic volume of gold nanorods can be calculated using the equation described below [178]:

$$V_h = \frac{4}{3}\pi \left(R_h\right)^3 = \frac{4}{3}\pi \left( \frac{L}{2 \ln\left(\frac{L}{d}\right) + q} \right)^3 \tag{5.4}$$

with $L$ the length of the nanorod, $d$ the diameter, and $q = 0.312 + 0.565(d/L) - 0.1(d/L)^2$.

Looking at the distribution of observed rotational diffusion times of single nanorods at 238 K in figure 5.5 (a), we observe a large dispersion, by a factor of about 3. Much of this dispersion of course arises from the large size distribution of the nanorods, obvious in the SEM image. This dispersion is a fundamental difference from single-molecule experiments. Individual probe molecules are all chemically identical, and therefore have exactly the same hydrodynamic volume. Variations in tumbling times for different molecules directly reflect variations in local viscosities. To compare rotational diffusion of different nanorods, however, we first have to get rid of the trivial variation in their hydrodynamic volumes.

Before estimating the volume dispersion, we have to consider two other possible sources of variation: (i) some nanorods may approach interfaces between glycerol and glass or air, and (ii) laser excitation may induce nanorod-dependent local heating. As the excitation light is focused into the liquid film with depth of about 1 $\mu m$, the nanorods in our confocal measurements are far from both interfaces. Gold nanorods can indeed cause local heating at moderate laser intensities due to their large absorption cross-section [183–185]. To exclude heating effects, we followed the rotational diffusion of several nanorods at different laser excitation powers at a given cryostat temperature (data not shown). From this measurement, we estimate the temperature rise due to local heating to be less than 0.02 K at the excitation intensity of 200 W/cm$^2$ at 633 nm, in good agreement with the calculated value 0.025 K based on the absorption cross-section [186,187]. Such small temperature rises are less than the uncertainty and stability in cryostat temperature. Furthermore, as the laser is applied throughout all measurements, variations of such small effects from rod

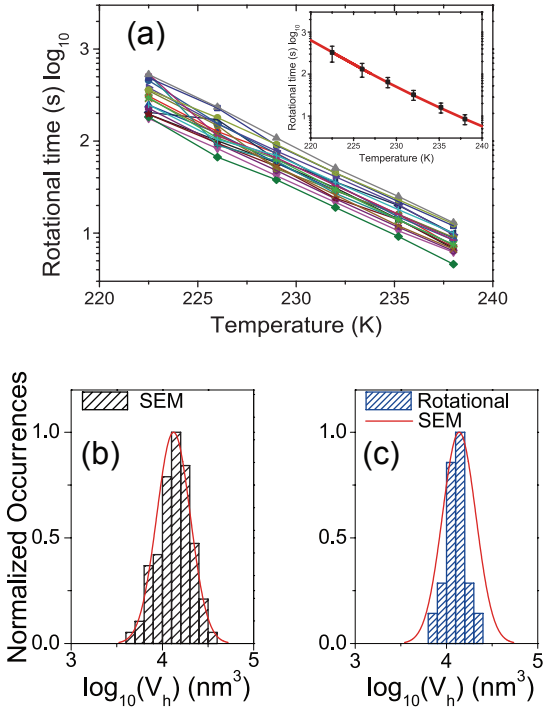


**Figure 5.5:** (a) Rotational correlation times of 19 individual gold nanorods against temperature. The inset shows the calculated values for 13 nm×33 nm nanorods (solid line) and the average values from 19 nanorods (black squares). (b) The histogram of nanorods' hydrodynamic volumes calculated using equation (5.4) from SEM measurements on 80 gold nanorods. The solid curve is the gaussian fit. The average hydrodynamic volume is (1.4±0.6) × $10^4$ $nm^3$. (c) The histogram of nanorods' hydrodynamic volumes deduced from rotational diffusion measurements on 19 nanorods at 238 K. It yield an average hydrodynamic volume of (1.1±0.4)×$10^4$ $nm^3$. The solid curve is the same as the one in (b).

to rod may safely be neglected. We thus mainly attribute the distribution of rotational times at 238 K to the volume distribution of gold nanorods. The average rotational time of 19 nanorods at 238 K is 8.5±2.3 seconds. This value is close to that calculated for a 13 nm×33 nm nanorod (8.4 seconds) at the same temperature, which is in a good agreement with the average dimension of 14±3 nm×35±5 nm from our SEM measurement, as shown in the inset of figure 5.5 (a).

This volume dispersion can be estimated in two independent ways. The

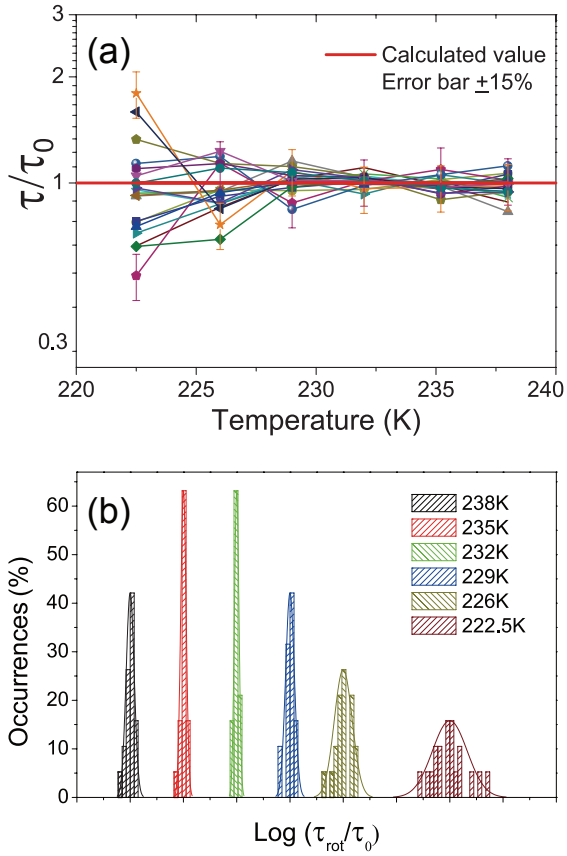


**Figure 5.6:** (a) The rotational times of the same 19 nanorods are normalized to their hydrodynamic volumes and to the bulk viscosity of glycerol. The hydrodynamic volume of each nanorod is fitted using equations (5.3) and (5.4) from its data points at 238 K, 235 K, and 232 K, where we do not see apparent broadening. After such normalization, we would expect a line ($\tau/\tau_0 = 1$, the red line) within the measurement uncertainty (error bar) if there was no heterogeneity. (b) Histograms of nanorods' rotational times, normalized to their volumes, at different temperatures. At 238 K, 235 K, 232 K and 229 K, distributions are narrow, broadened by experimental error only. Below 226 K, distributions clearly broaden.

SEM micrograph gives a dispersion of ±50%, $(1.4\pm0.6)\times10^4\,\mathrm{nm}^3$, shown in figure 5.5 (b). A second estimate is obtained by assuming that dynamical heterogeneity of glycerol is negligible at the highest measured temperature, 238 K. This assumption allows us to relate the time distribution to the volume dis-

tribution. The volume distribution estimated from the rotational diffusion, as shown in figure 5.5 (c), gives a half-maximum of ±40%. The distribution is narrower than that measured from SEM images (the solid curve in figure 5.5 (c)). This difference in volume distribution is probably due to a bias towards particles with a significant absorption cross-section at the excitation wavelength used for photoluminescence imaging. The estimated hydrodynamic volume of $(1.1\pm0.4)\times10^4$ nm$^3$ is in good agreement with the SEM estimate. Therefore, in the following, we suppose that the distribution of tumbling times at the highest temperature (238 K) is exclusively due to volume dispersion. Previous studies have indicated that heterogeneity is probably absent from single-molecule measurements at 238 K [33, 58, 65, 148]. This assumption is further supported by observations at 235 K and 232 K, to be discussed below, which show no big change in the width of the tumbling time distribution. With this assumption, we will deduce the hydrodynamic volume of each rod from its tumbling time at the higher temperatures.

Rotational times normalized to the bulk viscosity of glycerol and to each nanorods' volume are plotted against temperature in figure 5.6 (a). The volume of each nanorod is fitted from the rotational times at 238 K, 235 K, 232 K and 229 K, neglecting any dispersion of the local viscosity in this temperature range. We use this procedure to reduce and also to characterize the uncertainty in our measurements. The whole variation in data points for temperatures above 229 K reflect the uncertainty of our measurements (±15%, see size of error bars in figure 5.6). Below 226 K, the tumbling times of several nanorods start to depart from the average by more than the measurement uncertainty. At 222.5 K, several tumbling times are more than 50% off the expected line based on the bulk viscosity. This leads to a broadening in the histogram of rotational times at this temperature, as shown in figure 5.6 (b). These observations unambiguously indicate deviations of the local viscosity of glycerol from the average, i.e., they are unmistakable signatures of dynamical heterogeneity. These deviations start to appear already at 226 K. It would be very interesting to see whether the distribution further broadens at still lower temperatures. However, it was difficult to follow such large nanorods at lower temperatures in our experiments, as this would have required days of measurements for each point. The 10 K gap in temperature between single-molecule experiments and this work could be filled in future experiments with still smaller nanorods, or with enhanced fluorescence experiments [73].

## 5.3 Discussion

The main result of this work is the evidence it gives for heterogeneity in a domain of surprisingly high temperatures. As heterogeneity is sometimes associated to the formation of nanocrystallites [74], let us briefly rule out this phenomenon in the present experiments. Firstly, the lowest temperature upon first cooling in this study was 222.5 K, more than 30 K above the glass transition of glycerol. Previous experiments of our group have shown that crystallization of glycerol critically depends on thermal history, and only takes place after long enough aging at 195 K [181]. Secondly, if crystal growth occurred and the critical nucleus size was exceeded, the sample would rapidly crystallize at the temperature of 230 K, or upon warming up, and the nanorods would soon be immobilized. Instead, the nanorods remained mobile at all times, even after the sample was cooled further and was aged at 205 K for 10 hours (data not shown). Hence, even if nanocrystals form transiently in our experiments, they never reach the critical nucleus size.

Let us now discuss the length and time scales of the heterogeneity as felt by the gold nanorods. The most unexpected conclusion of our work is that, below 230 K, dynamical heterogeneity is still apparent and pronounced on the length scale of nanorods (about 30 nm). This length presumably extends even further, up to the length scale a nanorod explores by translational diffusion during the measurement. This is typically 10 times the rod's dimensions, as typical traces were recorded for about 100 reorientations. These distances are more than 30 times larger than earlier estimates of the length scales for dynamical heterogeneity in supercooled liquids, some nanometers [63,164,188]. Our results thus show for the first time that dynamical heterogeneity not only persists at the scale of a large dye molecule (one nanometer), but is still not averaged out over distances of several tens of nm. Presumably, the length scales of heterogeneity may extend even further, as there was no fundamental reason for the choice of this particular size of nanorods. Future experiments with larger rods will be undertaken to answer this question.

We now turn to the time scale of the heterogeneity. Even after an integration time of hours, heterogeneity was not time-averaged. This proves that the exchange times for fluctuations with correlation lengths comparable to the rod's size have to be comparable to, or longer than, 100 times the rod's tumbling time. When translated into the tumbling time of individual glycerol molecules, this time corresponds to more than $10^7$ tumbling steps of a glycerol molecule. It thus appears no longer relevant to discuss relaxation of heterogeneity at such large scales in terms of molecular tumbling times. Such long times would rather correspond to correlated rearrangements of a large

number of molecules, in so-called cooperatively rearranging regions (CRR's). These observations remind us of earlier findings by Patkowski *et al.* [171], who found large-scale, long-lived density fluctuations in glass-forming liquids. From small-angle X-ray scattering, they found a wide distribution of length scales, which led them to describe these structures as fractal. Such structures present heterogeneity at all length scales, and presumably also show wide distributions of relaxation times.

Our second key finding is the disappearance of heterogeneity when temperature is raised above 230 K. This value matches an earlier estimate by Zondervan *et al.* [58] based on observations of single dye molecules at temperatures between 205 and 212.5 K. We may tentatively identify this transition temperature with the critical temperature of mode coupling theory [67, 68], at which the relaxation time of the slowest fluctuation mode diverges. This temperature is expected to lie around 230 K for glycerol [53]. We can thus speculate on a possible scenario for the emergence of heterogeneity upon cooling down. When the first slow mode "freezes in" and leads to a long-lived density fluctuation, different regions of the glass-forming liquid cannot equilibrate any more, even after arbitrarily long waiting times. The way is then free for heterogeneities to develop independently from each other as temperature is lowered further, eventually leading to the dynamical mosaic of the low-temperature glass. The coincidence of this transition to heterogeneous behavior as observed on different length scales, from those of molecules to those of nanoparticles, is a strong indication that heterogeneity appears at various length scales simultaneously, i.e., at the same temperature or in a narrow range of temperatures.

Our results add to a large body of literature that conveys a view of glass-forming liquids as very complex and flexible systems. Depending on the thermal history of the sample, large structures up to microns can form [61,148,189], which can be imaged by fluorescence of dye impurities. It is natural to assume that similar structures can form on sub-micron scales too. It would be interesting to image them by superresolution microscopy [190–192], although the high doping densities required by these techniques might perturb the intrinsic structure of the pure glass-forming liquid. Using single molecules and single nanoparticles, as done here, has the advantage that the concentration of probes is so low that probe-probe interactions are negligible. Therefore, by comparing different individual probes with each other, one effectively removes the effect of probe-host interactions and one can concentrate on differences that must arise from the host itself.

## 5.4 Conclusion

We have demonstrated the first application of individual gold nanorods as local viscosity reporters in a supercooled liquid (glycerol) in a new range of temperatures (from 238 K to 222.5 K). The average rotational times agree very well with calculations based on the bulk viscosity of glycerol in that temperature range. After removing the trivial effect of the volume distribution of gold nanorods, we found that their rotational dynamics present clear differences from nanorod to nanorod in their temperature dependences. In this first study on 19 nanorods, cooling from 238 K to 222.5 K led to a significant distribution of local viscosities at temperatures lower than about 225 K. This result is surprising, because our nanorods are much larger (length 33 nm, diameter 13 nm) than the dye molecules used in previous studies. Moreover, because rotational diffusion times scale with volume, heterogeneity still survives averaging over very long times, several million times longer than molecular rotation times. The existence of such long memory times indicates that rearrangements must involve correlated motions of many molecules, in so-called cooperatively rearranging regions. Our results qualitatively match earlier observations of heterogeneity done on single molecules on shorter length scales and at lower temperatures, up to 212.5 K. For a quantitative comparison, it would be interesting to bridge the two temperature domains and to follow the development of dynamical heterogeneity over a temperature range including the homogeneous liquid at high temperature and the glassy mosaic at low temperature. However, it is difficult to follow rotational diffusion of these large gold nanorods at lower temperatures because their tumbling becomes extremely slow for the serial measurements done here. Parallel measurements of many rods simultaneously [59, 147, 193] would be a big advantage in this respect. To fill the temperature and dimension gap between this work and previous single-molecule experiments, using smaller gold nanorods would be an obvious solution. Alternatively, one could look at the rotational and translational diffusion of single dye molecules near plasmonic nanostructures, as was recently demonstrated with gold bowtie antennas [72] and gold nanorods [73]. Whichever way the study of glass formers will develop, dynamical heterogeneity is the central feature that has to be characterized and understood. Its unsuspected extent in space and time demonstrates once again the capacity of the nanoworld to surprise us by its intricacy and subtlety.

## Acknowledgements

H.Y., S.K., and M.O. acknowledge financial support from the European Research Council (Advanced Grant SiMoSoMa). P.Z. acknowledges financial support from the Netherlands Organization for Scientific Research (Veni Fellowship).